Available online at www.sciencedirect.com
SCIENCE DIRECT
Journal of Molecular Catalysis A: Chemical 255 (2006) 184–192
JOURNAL OF MOLECULAR CATALYSIS A: CHEMICAL
www.elsevier.com/locate/molcata

Study of Ga modified $Cs_{2.5}H_{1.5}PV_1Mo_{11}O_{40}$ heteropolyoxometallates for propane selective oxidation

Nikolaos Dimitratos [a], Jacques C. Védrine [b,*]

[a] *Dipartimento di Chimica Inorganica Metallorganica e Analitica e INSTM Unit, Centre of Excellence CIMAINA, Università di Milano, via Venezian 21, I-20133 Milano, Italy*
[b] *Laboratoire de Physico-Chimie des Surfaces, ENSCP, 11, rue P. & M. Curie, F-75005 Paris, France*

Received 25 February 2006; received in revised form 28 March 2006; accepted 29 March 2006
Available online 15 May 2006

Abstract

The selective oxidation of propane by oxygen has been investigated on a series of gallium modified $Cs_{2.5}H_{1.5}PV_1Mo_{11}O_{40}$ samples, with Ga content varying from 0 to 0.32 per Keggin unit (KU). The physicochemical properties of the samples have been studied by using a variety of techniques, namely ICP, FTIR, XRD, ^{31}P-NMR, BET and TG-DTG-DSC. The effect of several parameters, such as pre-treatment temperature, reaction temperature, residence time (W/F) on the conversion and product distribution has been examined. The presence of gallium has been observed to increase surface area by a factor of more than two and to improve the selectivity to oxygenates (acrylic and acetic acids, acrolein). It has been found that there is an optimum value of Ga content of 0.16 per KU in the Keggin structure and of pre heating temperature of 300 °C for maximizing propane conversion and acrylic acid selectivity. The latter aspect is related to the presence of both Brønsted acid and redox sites.

Keywords: Propane selective oxidation; Keggin Mo polyoxometallate compounds; $Cs_{2.5}$ HPA salts; Role of gallium

1. Introduction

Selective oxidation of light alkanes (C_1–C_5) is of growing interest and importance from both the industrial and the academic communities. The reason for this interest is due to the lower price and larger availability of light alkanes with respect to the corresponding alkenes [1–6] but also for a fundamental aspect of their activation as they are chemically much less active than the olefins. Heteropolyoxometallates have been used successfully for partial oxidation reactions. For instance a process has been developed for isobutene to methacrolein oxidation [7]. The interest of such materials is related to both their acidic and redox properties, which could be controlled, either by substituting the constituent elements or/and by partially exchanging the protons by redox metal cations [8–10]. Many articles have been published on catalytic performances of such compounds on partial oxidation of alkanes. It has been shown that the catalytic performance and thermal stability are enhanced by incorporating V^{5+} in the $H_3PMo_{12}O_{40}$ Keggin structure and by partial exchanging protons with Cs^+ cation. Moreover, addition of redox metals such as Fe, Ni, and Cu has been shown to substantially increase the formation of oxygenated products [11–18]. It has been suggested that the redox elements play an important role in the redox processes as reservoirs for electrons and active sites for the activation of hydrocarbons and molecular oxygen [19,20].

In a previous work we had studied the effect of redox elements (Ni, Co, Sb, Fe, Zn and Ga) substituting Mo cations on the acid and redox properties of heteropoly compounds [21]. In the present work we have studied the effect of Ga as a modifier of $Cs_{2.5}H_{1.5}PV_1Mo_{11}O_{40}$ compounds, as Ga is known to be a dehydrogenating element and has been used for propane and butane aromatisation to benzene and xylenes, respectively (cyclar process) [22–24] or for propane oxydehydrogenation on Ga/ZSM5 [25] or for propane ammoxidation on Ga/ZSM5 [26].

2. Experimental

2.1. Catalyst preparation

$H_4PVMo_{11}O_{40}$ sample was synthesized as follows. In a 500 cm^3 round bottom flask, 250 cm^3 of distilled water was

* Corresponding author. Tel.: +33 146 335 587; fax: +33 146 340 753.
E-mail address: jacques-vedrine@enscp.fr (J.C. Védrine).

1381-1169/$ – see front matter © 2006 Elsevier B.V. All rights reserved.
doi:10.1016/j.molcata.2006.03.075

added. Then the desired amounts of V_2O_5, MoO_3 and H_3PO_4 (85 wt.%) were added in the solution, until the desired stoichiometry was achieved. The solution was maintained at reflux for 24 h. The mixture was converted to a clear orange-red solution and was evaporated for the removal of water until dryness at 50 °C. The powder sample was collected and dried in vacuo overnight at 120 °C.

For the Ga_x-$Cs_{2.5}H_yPV_1Mo_{11}O_{40}$ samples, the $H_4PVMo_{11}O_{40}$ sample was dissolved in an aqueous solution and the desired amount of $Ga^{3+}(NO_3)_3$ was added (pH of 2), followed by the addition of a stoichiometric amount of Cs_2CO_3 at 50 °C. The resulting precipitate was evaporated to dryness at 50 °C and the powder was collected and was further dried at 120 °C in vacuo. The amount of Ga^{3+} added was in the range of 0.08–0.32 per Keggin unit (KU).

2.2. Catalyst characterization

The catalysts were characterized using FTIR, XRD, ICP, TG-DTG-DSC, BET and ^{31}P-NMR techniques. FTIR spectra of the samples were obtained using a Nicolet NEXUS FT-IR spectrometer (spectral range down to 400 cm^{-1}, resolution 2 cm^{-1}). For the study of lattice vibrational bands the samples were diluted (ca. 2 wt.%) and finely ground with dried KBr. The diffuse reflectance mode was used. XRD data were collected at ambient temperature with a Philips PW 1050 X-ray diffractometer equipped with a Hilten Brooks generator using the Co K_α radiation.

The chemical composition of the samples was determined using a Spectro CIROS SOP 120 ICP atomic emission spectrometer. The values are expressed in the chemical formulae calculated per Keggin Unit (KU). Thermogravimetric analysis was performed using a Setaram TG-DSC 111 instrument. The samples were mounted in platinum crucibles and heated at 10 °C min^{-1} to 600 °C under flowing helium. BET surface area measurements were carried out at liquid nitrogen temperature using a Micromeretics ASAP 2000 equipment after outgassing the sample at 250 °C.

^{31}P solid-state NMR measurements were recorded on a Bruker Avance DSX400 spectrometer with a spinning frequency of 4 kHz. The solid samples were introduced in a zirconia rotor without being outgassed. Chemical shifts are referred to the ^{31}P peak ($I = 1/2$) of 85% H_3PO_4.

2.3. Catalytic testing

Propane oxidation reaction was carried out at atmospheric pressure in a conventional flow system equipped with a stainless steel fixed bed microreactor. The reactor tube was 27 cm long and 2 cm i.d., placed vertically with a mesh in order to hold the catalyst at the same position in the isothermal part of the furnace. The control of the temperature was done, with a thermocouple placed in the centre of the tube reactor. The tube reactor was connected with mass flow controllers in order to provide the desired feed composition of gases (propane, oxygen, and helium). The effluents were analysed by GC chromatography (Varian CP 3800 model). The tubing system was heated at a temperature of 200 °C in order to avoid the polymerisation of the products. Due to the variety of possible products formed from the oxidation of propane, three different columns were chosen. Molsieve 13X (for O_2, CO and CH_4), HaysepD (for CO_2 and hydrocarbons) and FFAP for hydrocarbons. The first two columns were connected with a thermal conductivity detector (TCD) and the third one was connected with a Flame Ionisation Detector (FID). Prior to the reaction each catalyst was treated in an O_2 stream (30 cm^3 min^{-1}) at 300 °C or at 400 °C for 2 h in order to study the effect of the pre-treatment temperature. The feed consisted of 40 vol.% propane, 20 vol.% oxygen and He as balance. Note that water was not added to the feed. Total flow rates were varied from 7.5 to 30 cm^3 min^{-1} to study the effect of contact time. Reported values are given after 4 h of reaction under steady state unless otherwise stated.

3. Results and discussion

3.1. Characterization of $H_4PVMo_{11}O_{40}$ and Ga_x-$Cs_{2.5}H_yPVMo_{11}O_{40}$ compounds

3.1.1. FT-IR analysis

IR spectra of Keggin-heteropolyacids show four main bands, which are typically bands representing the Keggin unit [27,28]. These peaks have been assigned previously [9] and correspond for the first peak at 1080–1060 cm^{-1} to the ν_{as} (P-O_a) vibration mode, the second peak at 990–960 cm^{-1} to the ν_{as} (Mo-O_d) vibration mode, the third peak at 900–870 cm^{-1} to the ν_{as} (Mo-O_b-Mo) vibration mode and the fourth peak at 810–780 cm^{-1} to the ν_{as} (Mo-O_c-Mo) vibration mode. The subscripts indicate oxygen bridging Mo and the P heteroatom (a), corner-sharing (b) and edge-sharing (c) oxygen belonging to MoO_6 octahedra, and terminal oxygen (d).

The positions of the bands in the spectra also provide additional information on the composition of the Keggin unit. It has been reported [29] that incorporation of V^{5+} ion in the Keggin structure leads to a shift of the frequencies with respect to $H_3PMo_{12}O_{40}$. Specifically, when V^{5+} is incorporated in the acid form (0 to 3 per Keggin unit), ν_{as}(P-O_a) decreases from 1064 to 1059 cm^{-1}, ν_{as}(Mo-O_b-Mo) from 868 to 862 cm^{-1}, ν_{as}(Mo-O_c-Mo) from 789 to 783 cm^{-1} while ν_{as}(Mo-O_d) remains about constant at ca. 962 cm^{-1}.

IR spectra of Ga_x-$Cs_{2.5}H_yPVMo_{11}O_{40}$ samples, with x varying from 0 to 0.32, are shown in Figs. 1 and 2, before and after catalytic reaction, respectively. Replacing protons by Cs^+ cation induced a slight shift in the position of the characteristic peaks of the Keggin structure, as it is shown in Table 1. Particularly, an increase of the ν_{as} (M-O_d) and ν_{as} (M-O_c-M) (862–870 cm^{-1}) bands was observed, whereas the other two bands were affected only slightly. This shift is due to the strengthening of the M-O_d bond as the protonated water clusters are substituted by Cs cations [30]. New bands appeared at 997, 1037 and 1076 cm^{-1} as shoulders. The band at 997 cm^{-1} has been ascribed to the presence of MoO_3 [31], that at 1037 cm^{-1} to V_2O_5 or $(VO)^{2+}$ at exchangeable position, i.e. due to the release of V^{5+} from the structure [16,28], whereas that at 1076 cm^{-1} indicates the presence of vanadium in the Keggin oxoanion [32]. Finally,

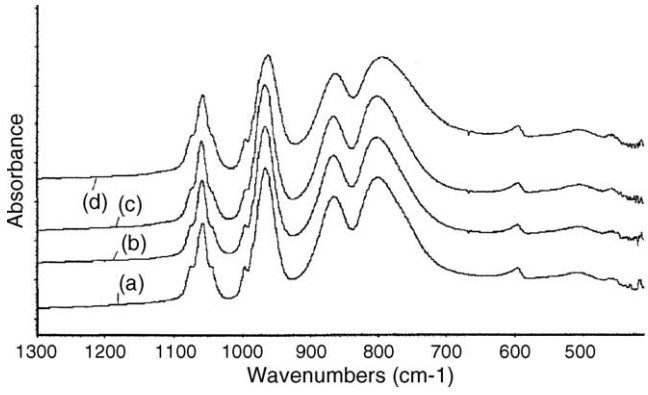

Fig. 1. FT-IR spectra of $Cs_{2.5}H_{1.5-3x}Ga_xPVMo_{11}O_{40}$ compounds. (a) Ga_0-$Cs_{2.5}H_{1.5}PVMo_{11}O_{40}$, (b) $Ga_{0.08}$-$Cs_{2.5}H_yPVMo_{11}O_{40}$, (c) $Ga_{0.16}$-$Cs_{2.5}H_yPVMo_{11}O_{40}$, (d) $Ga_{0.32}$-Cs_2. before catalytic reaction.

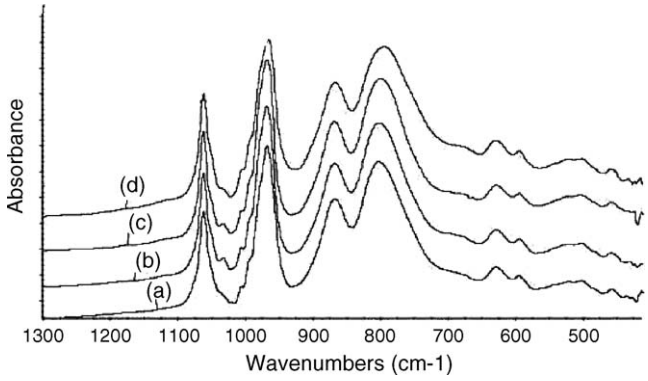

Fig. 2. FT-IR spectra of Ga_x-$Cs_{2.5}H_yPVMo_{11}O_{40}$ compounds. (a) Ga_0-$Cs_{2.5}H_{1.5}PVMo_{11}O_{40}$, (b) $Ga_{0.08}$-$Cs_{2.5}H_yPVMo_{11}O_{40}$, (c) $Ga_{0.16}$-$Cs_{2.5}H_yPVMo_{11}O_{40}$, (d) $Ga_{0.32}$-$Cs_{2.5}H_yPVMo_{11}O_{40}$ after catalytic reaction (heat pre-treatment at 400 °C).

Ga addition didn't affect the position and intensities of these shoulders appreciably up to 0.16 Ga/KU, showing that Ga is at exchangeable position, replacing protons or Cs^+ cation and not in the Keggin structure, while all frequencies decreased for higher Ga contents except ν_{as}(P-O_a) as if some of the Ga has been incorporated in the structure.

IR spectra of the used catalysts after pre-treatment temperature at either at 300 or 400 °C, showed that the Keggin structure was mainly maintained with some very small modifications. For used catalysts after catalytic reaction (Fig. 2) the intensity of the shoulder at 1076 cm^{-1} almost vanished whereas that of the shoulder 1037 cm^{-1} increased slightly, thus indicating that segregation of vanadium atoms from the primary structure of the oxoanions occurred during the reaction [29].

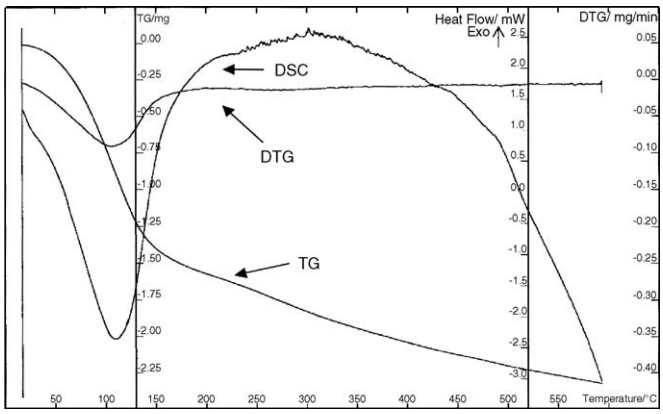

Fig. 3. TGA, DTG and DSC curves of $Ga_{0.08}$-$Cs_{2.5}H_yPVMo_{11}O_{40}$ sample.

3.1.2. TG-DTG-DSC analysis

TG-DTG-DSC analysis can provide information about the thermal stability and the number of crystallization and constitutional water molecules (number of protons attached with the polyanion) [33]. In our case the experimental values for $H_4PVMo_{11}O_{40}$ and $Cs_{2.5}H_{1.5}VMo_{11}O_{40}$ were close to the theoretical ones (3.9 and 2.0 against 4 and 1.5, respectively), indicating that V was incorporated in the Keggin structure (Table 2). At variance when Ga was added the experimental values obtained (3.0–3.4) are far from the theoretical ones if we assume that Ga^{3+} or $Ga(OH)^{2+}$ or $Ga(OH)_2{}^+$ have exchanged the protons, the latter Ga cationic species being favoured at low pH solution as shown by Bénézeth et al. [34], who have observed that the distribution of Ga cationic species (Ga^{3+}, $Ga(OH)^{2+}$, $Ga(OH)_2{}^+$, $Ga(OH)_3{}^0$ and GaO^+) in aqueous solution depends on the pH and temperature.

The endothermic peaks between 25 and 200 °C correspond to desorption of physisorbed water whereas some endothermicity between 200 and 500 °C corresponds to the desorption of constitutional water [21]. A typical TG-DTG-DSC curves for $Cs_{2.5}H_{1.5}PV_1Mo_{11}O_{40}$ sample is given in Fig. 3. TG analysis shows that addition of Cs^+ has a beneficial effect on the thermal stability of the samples, (Table 2). In addition, comparison of the theoretical values of constitutional protons with the experimental obtained can give us information about Brønsted acidity (Table 2). It is interesting to note that addition of Ga^{3+} resulted initially to an enhanced value and then to a plateau at higher Ga

Table 1
IR data in cm^{-1} of $H_yPV_xMo_{12-x}O_{40}$ and Ga_x-$Cs_{2.5}H_yPVMo_{11}O_{40}$ before catalytic reaction

Heteropoly compounds	ν_{as}(P-O_a) ±2 cm^{-1}	ν_{as}(Mo-O_d) ±2 cm^{-1}	ν_{as}(Mo-O_b-Mo) ±5 cm^{-1}	ν_{as}(Mo-O_c-Mo) ±5 cm^{-1}
$H_3PMo_{12}O_{40}$	1064	962	868	789
$H_4PV_1Mo_{11}O_{40}$	1063	962	867	785
Ga_0-$Cs_{2.5}H_{1.5}MoPVMo_{11}O_{40}$	1060 (1076[a], 1037[a])	970 (997[a])	868	802
$Ga_{0.08}$-$Cs_{2.5}H_yPVMo_{11}O_{40}$	1061 (1077[a], 1037[a])	969 (997[a])	868	803
$Ga_{0.16}$-$Cs_{2.5}H_yPVMo_{11}O_{40}$	1062 (1076[a], 1037[a])	970 (997[a])	868	803
$Ga_{0.32}$-$Cs_{2.5}H_yPVMo_{11}O_{40}$	1061 (1076[a], 1037[a])	965 (997[a])	865	796

[a] Indicates the presence of shoulders.

Table 2
TGA and BET data of Ga_x-$Cs_{2.5}H_yPVMo_{11}O_{40}$ samples

Heteropoly compounds	Temperatures of endothermic peaks (°C)	H^+/KU*	Temperatures of exothermic peaks (°C)	S.A (B.E.T) m^2g^{-1}		
				Fresh	After reaction PT of 300 °C	After reaction PT of 400 °C
$H_4PVMo_{11}O_{40}$	25–200, 200–380	3.9	410	6	–	–
Ga_0-$Cs_{2.5}H_{1.5}PVMo_{11}O_{40}$	25–200, 200–450	2.0	n.o	33	10	4
$Ga_{0.08}$-$Cs_{2.5}H_yPVMo_{11}O_{40}$	25–200, 200–450	3.4	n.o	73	12	4
$Ga_{0.16}$-$Cs_{2.5}H_yPVMo_{11}O_{40}$	25–200, 200–450	3.0	n.o	76	14	5
Ga_0.32-$Cs_{2.5}H_yPVMo_{11}O_{40}$	25–200, 200–450	3.1	n.o	73	15	5

PT stands for pre-treatment temperature. *Measured as water weight loss between 200 and 450 °C. n.o means no exothermic peaks were observed.

content, where the opposite trend was expected to happen. Our results are in agreement with those of Okuhara et al and of Langpape et al [9,35]. An explanation can be that Ga^{3+} species exists on the surface on a hydroxide form, [$Ga(OH)^{2+}$ or $Ga(OH)_2{}^+$], presumably the latter form at low pH value used for the preparation, and which can act as active sites for the reaction, as it has been proposed in the case of Fe^{3+} for dried samples. At higher temperature, the transformation of these species starts to begin leading to Ga_2O_3, as has been reported by I. Nowak et al [36].

In Table 3 the amount of H^+, calculated from the water lost above 300 and 400 °C, respectively is assumed to represent H^+ and OH remaining at those temperatures. However, the number of constitutional water molecules determined by TGA is directly related to Brønsted acid site for the H-form [33], whereas for Cs and Ga-Cs forms some water molecules are adsorbed more strongly to these cations, which leads to an excess of constitutional water with respect to Brønsted acid sites alone, which makes the method not reliable to measure the number of Brønsted sites. As it is expected at higher temperature, a low amount of constitutional water (Table 3) has remained, thus suggesting nevertheless that a major loss of Brønsted acidity has occurred.

3.1.3. BET surface area measurement

Addition of Cs is known [9] to result in higher surface area values and in increased thermal stability of the heteropoly compound. Moreover, substitution of protons by transition metals in the Cs heteropoly salts may affect the surface area depending on the specific transition metal used [35]. In our case, we found that the surface area of Ga_x-$Cs_{2.5}$ samples remained practically unchanged when Ga content varied from 0.08 to 0.32 (Table 2) per KU and was more than twice that before Ga addition. A similar trend was observed in the case of Cu [35]. After 12 h under catalytic reaction the surface area has decreased appreciably as shown in Table 2 (two last columns), which may be due to mesopores blocking by carbonaceous residue deposit or some sintering.

Table 3
Number of constitutional protons H^+ per Keggin unit calculated from water weight loss between 300–450 and 400–450 °C

Heteropoly compounds	H^+/KU[a]	H^+/KU remaining at 300 °C	H^+/KU remaining at 400 °C
Ga_0-$Cs_{2.5}H_{1.5}PVMo_{11}O_{40}$	1.5	1.2	0.2
$Ga_{0.08}$-$Cs_{2.5}H_yPVMo_{11}O_{40}$	1.58	1.6	0.4
$Ga_{0.16}$-$Cs_{2.5}H_yPVMo_{11}O_{40}$	1.66	1.5	0.5
$Ga_{0.32}$-$Cs_{2.5}H_yPVMo_{11}O_{40}$	1.82	1.6	1.0

[a] Calculated from the chemical analysis assuming protons being exchanged by Ga cation as $Ga(OH)_2{}^+$ species.

3.1.4. X-ray diffraction analysis

The X-ray diffraction data obtained for the fresh Ga_x-$Cs_{2.5}$ compounds are illustrated in Fig. 4. Substitution of protons by Cs cations lead to the formation of a cubic phase (Pn3m) commonly associated with the alkaline heteropolysalts [9]. The addition of Ga did not modify the X-ray diffraction patterns. Moreover, calculation of cell parameters of the cubic phase showed no appreciable differences versus Ga loading. These results are in agreement with those reported by Langpape et al, studying Cu and Fe cations for the substitution of protons [35]. Thus, it can be concluded that addition of Ga neither affects nor even modifies the structure of the heteropolyacid. This matter is further supported by ^{31}P MAS-NMR data given below.

The XRD patterns of the used samples (not presented) did not show any detectable difference with the fresh ones. Free vanadium oxide species and α-MoO_3 (as observed from the IR spectra) were not detected due to their low amount and/or high dispersion.

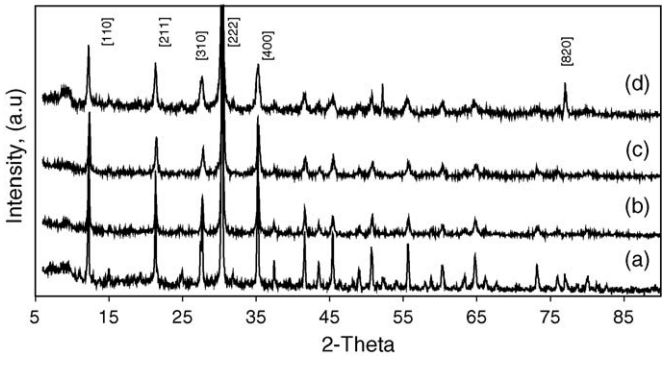

Fig. 4. XRD patterns of Ga_x-$Cs_{2.5}H_yPVMo_{11}O_{40}$ compounds before catalytic reaction. (a) Ga_0-$Cs_{2.5}H_{1.5}PVMo_{11}O_{40}$, (b) $Ga_{0.08}$-$Cs_{2.5}H_yPVMo_{11}O_{40}$, (c) $Ga_{0.16}$-$Cs_{2.5}H_yPVMo_{11}O_{40}$, (d) $Ga_{0.32}$-$Cs_{2.5}H_yPVMo_{11}O_{40}$.

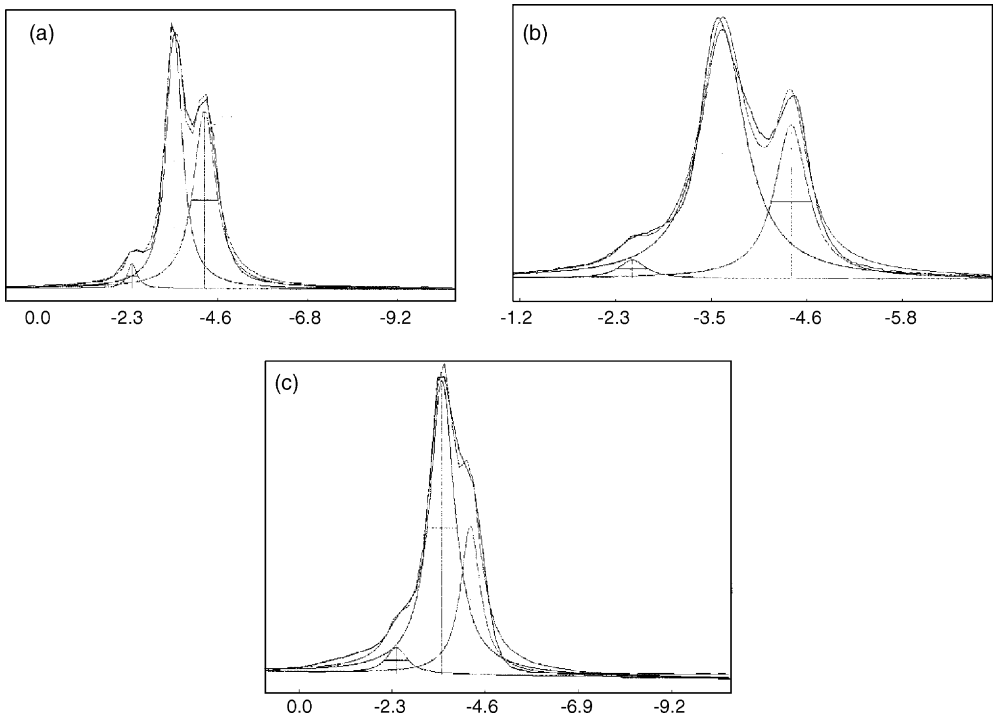

Fig. 5. ^{31}P-MAS NMR spectra for Ga_x-$Cs_{2.5}H_yPVMo_{11}O_{40}$ compounds before catalytic reaction, (a) Ga_0-$Cs_{2.5}H_{1.5}PVMo_{11}O_{40}$, (b) $Ga_{0.08}$-$Cs_{2.5}H_yPVMo_{11}O_{40}$, (c) $Ga_{0.32}$-$Cs_{2.5}H_yPVMo_{11}O_{40}$.

3.1.5. *^{31}P MAS-NMR analysis*

^{31}P MAS-NMR is a useful technique for providing information about the integrity of the primary structure of phosphorous-containing heteropolyacids and can evidence any changes in the chemical environment of phosphorous as a function of Ga addition and further on upon catalytic reaction conditions.

The ^{31}P MAS-NMR study was performed at room temperature without degassing the samples. Typical spectra for Ga_x-$Cs_{2.5}H_yPVMo_{11}O_{40}$ samples and their decomposition are presented in Fig. 5 and the main data are given in Table 4. The decomposition of the spectra resulted in three peaks (−2.4, −3.6 and −4.3 ppm). The peaks at −2.5 and −3.6 ppm have been assigned previously to dehydrated and hydrated $H_4PVMo_{11}O_{40}$ (see Table 4 in [33]) and the peak at −4.3 ppm to $Cs_4PV_1Mo_{11}O_{40}$. Ga addition did not shift appreciably the position of the corresponding peaks, but increased the −3.5 ppm peak intensity at the expense of the −4.3 ppm one, suggesting that some Ga has been incorporated into the Keggin anion, leading to more protons and thus more Brønsted acidity.

After catalytic reaction at 340 °C the ^{31}P MAS-NMR spectrum of 400 °C pre-treated $Ga_{0.08}$-$Cs_{2.5}H_yGaPV_1Mo_{11}O_{40}$ sample was recorded (Fig. 6). A large amount of the peak at −3.6 ppm (Table 5) has been lost (67% before catalytic reaction against 6% after), indicating that the majority of the acid $H_4PVMo_{11}O_{40}$ sample deposited on $Cs_4PVMo_{11}O_{40}$ has been dehydrated [33]. This result is quite in line with TGA study given above (§ 3.1.2).

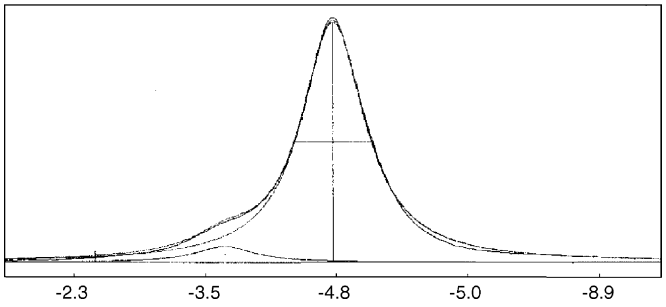

Fig. 6. ^{31}P-MAS NMR spectra for $Ga_{0.08}$-$Cs_{2.5}H_yPVMo_{11}O_{40}$ sample after 12 h of catalytic reaction.

3.2. *Catalytic study of calcined Ga_x-$Cs_{2.5}H_yPV_1Mo_{11}O_{40}$ samples*

Usually catalysts are calcined before reaction at temperatures higher than the operating temperature in the reactor to avoid any

Table 4
^{31}P-MAS NMR chemical shifts for Ga_x-$Cs_{2.5}H_yPVMo_{11}O_{40}$ compounds before catalytic reaction, $x = 0$, 0.08, 0.32

Heteropoly compounds	Chemical shift (ppm)
Ga_0-$Cs_{2.5}H_{1.5}PVMo_{11}O_{40}$	−2.4 (3%), −3.5 (49%), −4.3 (48%)
$Ga_{0.08}$-$Cs_{2.5}H_yPVMo_{11}O_{40}$	−2.6 (3%), −3.6 (67%), −4.4 (30%)
$Ga_{0.32}$-$Cs_{2.5}H_yPVMo_{11}O_{40}$	−2.4 (5%), −3.5 (67%), −4.2 (28%)

Table 5
^{31}P-MAS NMR chemical shifts for $Ga_{0.08}$-$Cs_{2.5}H_yPVMo_{11}O_{40}$ compounds after 12 h of catalytic reaction

Heteropoly compounds	Chemical shift (ppm)
$Ga_{0.08}$-$Cs_{2.5}H_yPVMo_{11}O_{40}$	−3.6 (6%), −4.6 (94%)

Table 6
Catalytic data after 4 h on stream for Ga_x-$Cs_{2.5}H_yPVMo_{11}O_{40}$ samples in the reaction temperature (T_{reac}) range 300–340 °C, contact time 2.1 s, flow rate 15 cm^3 min^{-1}, C_3:O_2:He = 40:20:40

Catalyst	T_{reac} (°C)	Treatment at 300 °C								
		Selectivities %								Conv. %
		CO	CO_2	CO_x	$C_3^=$	Ac.A[a]	A.A[a]	ACR[a]	Σ O_x.P	C_3
Ga_0-$Cs_{2.5}H_{1.5}PVMo_{11}O_{40}$-	300	12.4	9.7	22.1	52.8	22.4	0	2.7	25.1	3.4
	320	16.1	12.2	28.3	43.1	23.7	3.2	1.7	28.6	6.0
	340	15.3	11.2	26.5	38.5	28.2	2.4	3.5	34.1	9.9
$Ga_{0.08}$-$Cs_{2.5}H_{1.5}PVMo_{11}O_{40}$	300	18.4	10.8	29.2	25.5	26.7	15.8	2.8	45.3	2.1
	320	24.9	16.0	40.9	14.7	27.7	13.9	2.8	44.4	7.9
	340	27.9	19.1	47.0	17.3	21.7	11.1	2.9	35.7	12.8
$Ga_{0.16}$-$Cs_{2.5}H_{1.5}PVMo_{11}O_{40}$	300	19.2	14.4	33.6	21.7	28.7	13.6	2.4	44.7	8.7
	320	22.5	15.3	37.8	16.4	25.3	18.0	2.5	45.8	12.7
	340	22.5	16.4	38.9	16.3	22.4	20.0	2.4	44.8	18.1
$Ga_{0.32}$-$Cs_{2.5}H_{1.5}PVMo_{11}O_{40}$-	300	21.8	24.3	46.1	29.5	24.4	0	0	24.4	7.1
	320	22.5	24.6	47.1	20.5	25.5	4.9	2.0	32.4	11.2
	340	25.4	26.8	52.2	15.9	23.5	6.3	2.1	31.9	16.6

Preheating temperature 300 °C.
[a] C_3: propylene, AcA: acetic acid, AA: acrylic acid, ACR: acrolein, $CO_x = CO + CO_2$, Σ O_x.P = sum of oxygenated products (ACR, Ac.A and A.A).

thermal instability of the catalyst in this temperature domain. However, in many articles of the literature dealing with the study of HPA compounds for selective alkane oxidation, calcination of the catalysts was performed at lower temperatures than that of the reaction [9,16,37,38] to control the amount of Brønsted acid sites. In the present study, the catalysts have been calcined before reaction at two different temperatures, namely 300 and 400 °C and the catalytic study was performed between 300 and 400 °C and under propane-rich conditions, the latter choice to favour higher selectivity towards to oxygenated products [39] and without water in the feed.

3.2.1. Influence of reaction temperature

The catalytic study of propane oxidation on Ga_x-$Cs_{2.5}H_y$ $PV_1Mo_{11}O_{40}$ samples with x being varied between 0 and 0.32 was performed in the 300–400 °C temperature range. The main products were acrolein (ACR), acrylic acid (A.A), acetic acid (Ac.A), CO and CO_2. Fig. 7 and Table 6 illustrate the effect of reaction temperature on conversion and selectivities for $Ga_{0.08}$-$Cs_{2.5}H_yPVMo_{11}O_{40}$ taken as an example. The same trend was found for the whole series of Ga_x-$Cs_{2.5}H_yPVMo_{11}O_{40}$ catalysts. Principally the formation of CO_x products was enhanced substantially as a result of the increase in reaction temperature. Reaction temperature higher than 340 °C resulted in the increase of the conversion, but with substantial decrease in the formation of oxygenated products. These results indicated that an optimum reaction temperature for the formation of oxygenated products is 340 °C, temperature chosen for further studies.

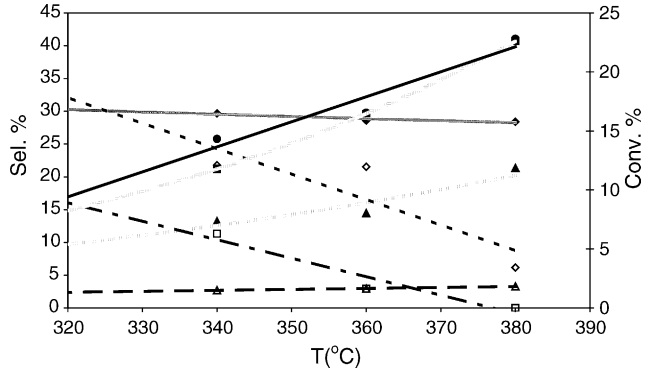

Fig. 7. Variations of propane conversion (●) and selectivities as a function of temperature for $Ga_{0.08}$-$Cs_{2.5}H_yPVMo_{11}O_{40}$ sample pre-treated at 300 °C with C_3:O_2:He = 2:1:2, total flow rate 15 cm^3 min^{-1}. Selectivity to CO (♦), CO_2 (■), $C_3^=$ (▲), Ac.A (◊), A.A (□), ACR (△).

3.2.2. Influence of contact time on Ga_x-$Cs_{2.5}H_yPV_1Mo_{11}O_{40}$ samples pre-treated at 400 °C

Experimental results on the effect of contact time are presented in Table 7 for $Ga_{0.16}$-$Cs_{2.5}H_yPVMo_{11}O_{40}$ taken as an example. By increasing the contact time, propane conversion increased, selectivity to propene and acrolein decreased, whereas selectivities to acetic acid and CO_x increased as could be expected for successive reactions (see reaction Scheme 1 described below). In the case of acrylic acid, the general trend was that an increase in selectivity was obtained by increasing the contact time reaching a maximum value followed then by a decline, suggesting that consecutive oxidation was happening in favour of CO_x formation. This trend for acrylic acid was observed only for the samples with Ga content equal or higher than 0.16. Note that substantial formation of acrylic acid was achieved, when Ga content was equal or higher than 0.16. Optimum contact time equal to 2.1 s was observed for all samples giving best A.A selectivity, all results for the other samples are not given here for clarity.

3.2.3. Ga_x-$Cs_{2.5}H_yPV_1Mo_{11}O_{40}$ samples pre-treated at 300 and 400 °C

Comparison of the catalytic data under the same reaction conditions (same contact time, of 2.1 s and same reaction tem-

Table 7
Catalytic data for $Ga_{0.16}$-$Cs_{2.5}H_yPVMo_{11}O_{40}$ compounds at 340 °C as a function of contact time, C_3:O_2:He = 40:20:40

Catalyst	Contact time (s)	Selectivity %								Conv. %
		CO	CO_2	CO_x	$C_3^=$	Ac.A[a]	A.A[a]	ACR[a]	Σ O_x.P	C_3
$Ga_{0.16}$-$Cs_{2.5}H_{1.5}PVMo_{11}O_{40}$-300	0.8	17.1	17.6	34.7	41.6	14.2	2.8	6.7	23.7	3.1
	1.0	16.2	14.2	30.4	41.3	16.5	6.7	5.1	28.3	5.8
	1.4	20.0	16.6	36.6	27.3	20.4	10.6	5.1	36.1	8.6
	2.1	22.8	17.1	39.9	20.2	22.9	12.9	4.1	39.9	9.5
	4.1	24.7	22.3	47.0	13.7	27.5	9.2	2.6	39.3	11.9

Preheating temperature 400 °C.
[a] C_3: propylene, Ac.A: acetic acid, A.A: acrylic acid, ACR: acrolein, $CO_x = CO + CO_2$, Σ O_x.P = sum of oxygenated products (ACR, Ac.A and A.A).

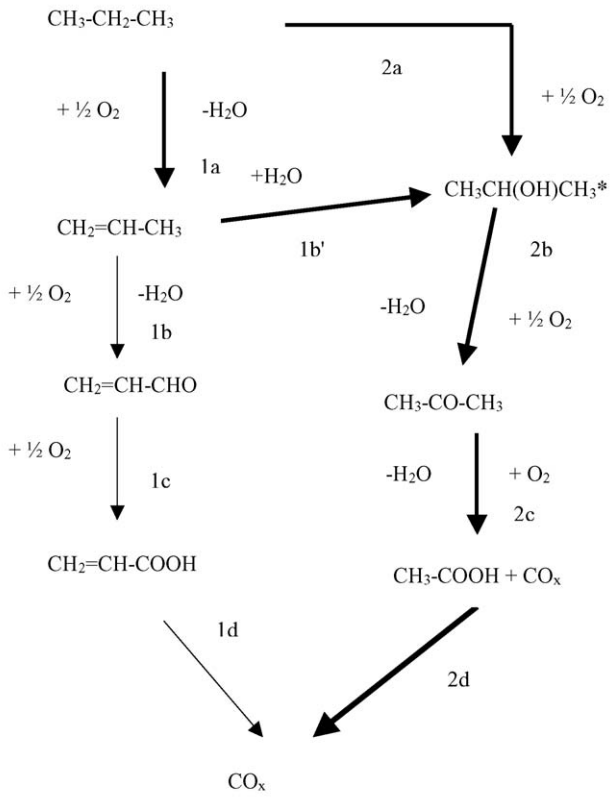

Scheme 1. Reaction pathways for propane oxidation on Ga_x-$Cs_{2.5}H_y$ $PVMo_{11}O_{40}$ samples. The thick arrows indicate the major pathway.

perature of 340 °C) for samples pre-heated at 300 and 400 °C is given in Table 8. Drop in the activity was observed after higher pre-treatment temperature, whereas in terms of selectivity no significant change was found for acetic acid. On the contrary, selectivity to acrylic acid showed a significant decrease at the profit of propene. Note that surface area values for both pre-treatment temperatures (see Table 2 and as reminded for clarity in Table 8) has decreased after reaction, as it has already been reported [40,41]. The decrease in catalytic activity after pre-treatment at higher temperature is therefore certainly related to the decrease in surface area.

3.2.4. *Effect of gallium content*

Formation of acrylic acid was observed when Ga was added to the HPA. It can be seen clearly that the introduction of Ga in the heteropolyacid samples has a beneficial effect in terms of activity, as an increase in conversion was observed, which is coherent with the increase in surface area values (Table 2). In terms of selectivity, a substantial increase in the selectivity to oxygenates, mainly acrylic acid was observed with a maximum obtained for $x = 0.16$/KU at the expense of propene.

When Ga content increased, selectivity to propene decreased substantially in favour of acrylic acid mainly, whereas selectivity to CO_x products increased mainly after 300 °C pre-treatment temperature. Note that only at Ga loading above 0.08, formation of acrylic acid was observed at both pre-treatment temperatures,

Table 8
Catalytic data for $Cs_{2.5}H_yGa_xPVMo_{11}O_{40}$ compounds at 340 °C, contact time 2.1 s, flow rate 15 cm^3 min^{-1}, C_3:O_2:He = 40:20:40 with pre-treatment temperature at 300 and 400 °C with surface area values after reaction in parentheses

Catalyst-Pre-treatment temperature °C	Selectivities %								C_3 Conv. % (S m^2 g^{-1})
	CO	CO_2	CO_X	$C_3^=$	Ac.A[a]	A.A[a]	ACR[a]	Σ O_x.P	C_3
Ga_0-$Cs_{2.5}H_{1.5}PVMo_{11}O_{40}$-300	15.3	11.2	26.5	38.5	28.2	2.4	3.5	34.1	9.9 (10)
Ga_0-$Cs_{2.5}H_{1.5}PVMo_{11}O_{40}$-400	26.1	16.9	43.0	28.7	25.5	0.0	2.8	28.3	11.2 (4)
$Ga_{0.08}$-$Cs_{2.5}H_yPVMo_{11}O_{40}$-300	27.9	19.1	47.0	17.3	21.7	11.1	2.9	35.7	12.8 (12)
$Ga_{0.08}$-$Cs_{2.5}H_yPVMo_{11}O_{40}$-400	21.2	20.6	41.8	28.4	23.9	0.0	5.9	29.8	9.9 (4)
$Cs_{2.5}H_yGa_{0.16}PVMo_{11}O_{40}$-300	22.5	16.4	38.9	16.3	22.4	20.0	2.4	44.8	18.1 (14)
$Cs_{2.5}H_yGa_{0.16}PVMo_{11}O_{40}$-400	22.8	17.1	39.9	20.2	22.9	12.9	4.1	39.9	9.5 (5)
$Cs_{2.5}H_yGa_{0.32}PVMo_{11}O_{40}$-300	25.4	26.8	52.2	15.9	23.5	6.3	2.1	31.9	16.6 (15)
$Cs_{2.5}H_yGa_{0.32}PVMo_{11}O_{40}$-400	23.1	20.4	43.5	18.8	25.1	9.7	2.9	37.7	9.7 (5)

[a] C_3: propylene, Ac A: acetic acid, A.A: acrylic acid, ACR: acrolein, $CO_x = CO + CO_2$, Σ O_x.P = sum of oxygenated products (ACR, Ac.A and A.A).

indicating that the presence of Ga is important as active sites responsible for the formation of acrylic acid. These results are in agreement with those of Okuhara et al. and Langpape et al. when Fe was the transition metal [9,42]. Finally, selectivity to acrylic acid was the highest for the lower pre-treatment temperature, while Brønsted acidity was different (Table 3). These results indicate that an optimum amount of redox element and a certain acidity have contributed at the same time not only on the activity but also on selectivity to acrylic acid. As seen in Scheme 1 and in agreement with our data discussed above, propane oxidation follows two main pathways. The first pathway is the oxidation of propane to propylene (1a) and consecutively to acrolein (1b), which further transforms to acrylic acid (1c) or the hydration of propylene leading to isopropyl alcohol (1b′). The second pathway (2) is the direct oxidation of propane to isopropyl alcohol (2a), which is further oxydehydrogenated to acetone (2a) and finally oxidised to acetic acid and CO_x (2c). One can then suggest that the role of acidity is not only to activate propane, but also to facilitate desorption of the acrylic acid from the surface, while the redox role of Ga element is to facilitate selective oxidation. However, control of the acidity is necessary due to the fact that a too high value can lead to the consecutive oxidation of acrylic acid to CO_x formation (1d) or to promotion of the formation of acetic acid through the isopropyl alcohol route by hydration of propylene on Brønsted acid sites (1b′) [33]. It can be concluded that Ga facilitates the promotion of the consecutive oxidation of propene to acrolein (1b), which is further transformed to acrylic acid (1c). Its redox properties, i.e. its reduction potential, when in the heteropolyoxometallate (POM), could be characterised by STM as shown by M. Barteau et al. on model POM systems [43], namely ordered HPA monolayers on graphite surface. In such experiments HPA with different heteroatoms were studied for their negative differential resistance (NDR) in the current–voltage (*I–V*) of the STM. Correlations could be established between reduction potentials and NDR peak voltages and with catalytic properties, namely less negative NDR peaks were associated with higher activity, while selectivity presented a maximum (volcano curves) [43]. For instance for propane to acrylic acid a maximum selectivity of 30% was obtained for NDR values around −0.75–0.5 V.

4. Conclusions

The present work has shown that Ga can be utilised as an effective counter-cation for promoting the selective oxidation of propane towards to acrylic acid. Depending on the amount of Ga in the heteropolyacid samples, a beneficial effect in terms of activity and selectivity to acrylic acid was found, with an optimum ratio for 0.16 Ga species per KU, which is similar to previous reported values for Fe [9,42]. Moreover, heat pre-treatment is affecting the activity and the product distribution, with a lower pre-treatment temperature of 300 °C resulting in higher formation of oxygenated products. Nevertheless, in both pre-treatment temperatures the beneficial role of Ga was shown. As a general conclusion it can be said that Ga addition and pre-treatment temperature permit to tune the Brønsted and redox sites amount and thus to favour acrylic acid formation at the expense of acetic acid or/and propene and/or CO_x.

References

[1] N. Mizuno, M. Misono, in: E.G. Derouane, et al. (Eds.), Catalytic Activation and Functionalization of Alkanes, Kluwer Academic Publ, Dordrecht, 1998, p. 311.
[2] F. Cavani, F. Trifirò, Stud. Surf. Sci. Catal. 110 (1997) 19.
[3] R.H. Crabtree, Chem. Rev. 95 (1995) 987.
[4] W.E. Slinkard, A.B. Baylis, US Patent 4192951 (1998). assigned to Celanese Corp.
[5] K. Kourtakis, US patent 5510308 (1996). assigned to Du Pont Co.
[6] K. Nowinska, M. Sopa, A. Wraclaw, D. Szuba, Appl. Catal. A: Gen. 225 (2002) 141.
[7] M. Matsumoto, K. Wada, A. Sudo, Eur. Patent. 5769 (1979). assigned to Nippon Kayaku Co.
[8] N. Mizuno, M. Misono, Chem. Rev. 98 (1998) 199.
[9] T. Okuhara, N. Mizuno, M. Misono, Adv. Catal. 41 (1996) 113.
[10] M.T. Pope, A. Müller, Angew. Chem. Int. Ed. Engl. 30 (1991) 34.
[11] M. Ai, Appl. Catal. 4 (1982) 245.
[12] N. Mizuno, H. Yahiro, J. Phys. Chem. B 102 (1998) 437.
[13] N. Mizuno, M. Tateishi, M. Iwamoto, J. Catal. 163 (1996) 87.
[14] H. Imai, T. Yamaguchi, M. Sugiyama, Jap. Patent 63145249 (1988). assigned to Asahi Chemical Industry Co.
[15] K. Nagai, Y. Nagaoka, H. Sato, M. Ohsu, Eur. Patent 0418657 (1991). assigned to Sumitomo Chemical Co.
[16] N. Mizuno, W. Han, T. Kudo, J. Mol. Catal. A: Chem. 114 (1996) 309.
[17] T. Kuroda, M. Ohkita, Eur. Patent 0543019 (1993). assigned to Mitsubishi Rayon Co.
[18] M.T. Pope, Heteropoly and Isopoly Oxometalates, Springer, Berlin, 1983, p. 93.
[19] S. Albonetti, F. Cavani, F. Trifirò, Catal. Rev. Sci. Eng. 38 (1996) 413.
[20] E. Cadot, C. Marchal, M. Fournier, A. Tézé, G. Hervé, in: M.T. Pope, A. Müller (Eds.), Polyoxometalates, Kluwer Academic Publishers, Dordrecht, 1994, p. 315.
[21] N. Dimitratos, J.C. Védrine, Catal. Today 81 (2003) 561.
[22] R. Gregory, A.J. Colombos, US patent 4056575 (1977). assigned to British Petroleum Co.
[23] S.N. Bulford, E.E. Davie, US patent 4157356 (1979). assigned to British Petroleum Co.
[24] J.R. Mowry, R.F. Anderson, J.A. Johnson, Oil Gas J. 2 (1985) 128.
[25] V. Cortés Corberan, R.X. Valenzuela, B. Sulikowski, M. Derewinski, Z. Olejniczak, J. Krysciak, Catal. Today 32 (1996) 193.
[26] P. Pal, J. Quartararo, S.B. Abd Hamid, E.G. Derouane, J.C. Védrine, P.C.M.M. Magusin, B.G. Anderson, Can. J. Chem. 83 (2005) 574.
[27] C. Rocchiccioli-Deltcheff, M. Fournier, R. Franck, R. Thouvenot, Inorg. Chem. 22 (1983) 207.
[28] C. Rocchiccioli-Deltcheff, M. Fournier, J. Chem. Soc. Faraday Trans. 87 (1991) 3913.
[29] J.K. Lee, J. Melsheimer, S. Berndt, G. Mestl, R. Schlögl, K. Köhler, Appl. Catal. A: Gen. 214 (2001) 125.
[30] N. Essayem, A. Holmqvist, P.Y. Gayraud, J.C. Védrine, Y. Ben Taârit, J. Catal. 197 (2001) 273.
[31] S. Damyanova, J.L.G. Fierro, Chem. Mater. 10 (1998) 871.
[32] G. Centi, V. Lena, F. Trifiro, J. Chem. Soc. Faraday Trans. 86 (1990) 2775.
[33] N. Dimitratos, J.C. Védrine, Appl. Catal. A: Gen. 256 (2003) 251.
[34] P. Bénézeth, I.I. Diakonov, G.S. Pokrovski, J.-L. Dandurand, J. Schott, I.L. Khodakovsky, Geochem. Cosmochim. Acta 61 (1997) 1345.
[35] M. Langpape, J.M.M. Millet, U.S. Ozkan, M. Boudeulle, J. Catal. 181 (1999) 80.
[36] I. Nowak, J. Quartararo, E.G. Derouane, J.C. Védrine, Appl. Catal. A: Gen. 251 (2003) 107.

[37] N. Mizuno, M. Tateishi, M. Iwamoto, Appl. Catal. A: Gen. 118 (1994) L1.
[38] N. Mizuno, M. Tateishi, M. Iwamoto, Appl. Catal. A: Gen. 128 (1995) L165.
[39] F. Cavani, F. Trifiro, Catal. Today 51 (1999) 561.
[40] M. Langpape, J.M.M. Millet, Appl. Catal. A: Gen. 200 (2000) 89.
[41] F. Cavani, M. Koutyrev, F. Trifiro, Catal. Today 28 (1996) 319.
[42] M. Langpape, J.M.M. Millet, U.S. Ozkan, P. Delichère, J. Catal. 182 (1999) 148.
[43] M.A. Barteau, J.E. Lyons, I.K. Song, J. Catal. 216 (2003) 236.